

A Novel Direct Control of Z-Source Inverter Based on Adaptive Neuro-Fuzzy Inference System

Dr. Majid K. Al-Khatat

Electrical Engineering Department, University of Technology/Baghdad.

Lina J. Rashad

Electrical Engineering Department, University of Technology/Baghdad.

Email: lina.j.rashad@gmail

Received on:12/3/2015 & Accepted on:17/9/2015

ABSTRACT

This paper proposes a novel method for controlling the output DC-link voltage of the Z-source inverter for adjustable speed drive applications. An adaptive neuro-fuzzy controller is used to control the DC-link. The novelty of the proposed controller is the direct feedback from the DC-link, which is a discontinuous (chopped) signal, without any additional estimation or peak detection circuits. Where, this discontinuous feedback can't be used in conventional controllers without additional circuits. Design and simulation of the proposed control system are illustrated in this paper. Simulation results give excellent performance of the Z-source inverter with ripple free DC-link voltage. The robustness of the proposed intelligent controller is demonstrated for different output voltage commands. The response of the DC-link voltage, output AC voltage, AC current and speed for 20% and 40% input voltage sag is investigated.

Keywords: Z-source inverter, direct control, ASD system, ANFIS control, intelligent control.

السيطرة المباشرة على عاكس مصدر-الممانعة استناداً على نظام الاستدلال العصبي-
الضبابي المكيف

الخلاصة

تقترح هذه الورقة طريقة جديدة للسيطرة على جهد وصلة-التيار المستمر (DC-link voltage) لعاكس مصدر الممانعة في تطبيقات مسواقات السرعة المتغيرة. تم استخدام وحدة التحكم العصبي-الضبابي المكيف للسيطرة على جهد وصلة-التيار المستمر. الجديد بوحدة التحكم المقترحة هو استخدام التغذية الخلفية المباشرة من وصلة-التيار المستمر والتي تتصف بعدم الأستمرارية (متقطعة), وذلك بدون أي استخدام لدوائر تقييم أو كشف عن الذروة. حيث ان هذه التغذية الخلفية غير المستمرة لا يمكن أن تستخدم في المسيطرات التقليدية دون استخدام دوائر اضافية. في هذه الورقة تم توضيح التصميم والمحاكاة لنظام السيطرة المقترح. نتائج المحاكاة اعطت أداءً ممتازاً لعاكس مصدر-الممانعة مع جهد وصلة-التيار المستمر خالي من التموج. كما وتمت برهنة متانة وحدة التحكم الذكية المقترحة لمختلف اوامر انتاج الجهد الكهربائي. وتم تقصي استجابة جهد وصلة-التيار المستمر والجهد والتيار المتناوبين الناتجين والسرعة لأنخفاض بمقدار 20% و40% بجهد الأذخال.

INTRODUCTION

In 2003, Fang Zheng Peng introduced a new type of impedance source power converter (Z-source converter) [1]. Fig. (1) shows the ZSI structure which employs a unique impedance network to couple the converter main circuit to the power source, load, or another converter, for providing unique features that cannot be observed in the traditional V- and I-source converters where a capacitor and inductor are used respectively such as: provides a greater voltage than the input voltage, improves the input power factor, reduces the inrush current & harmonics in the current because of two inductors in Z-source network, forms a second order filter and handles the undesirable voltage sags of the DC voltage source [2], [3]. The ZSI can buck & boost the DC voltage by using the shoot through operating mode, two switches in the same phase legs can be gated on simultaneously, and without DC/DC converter or bulky transformers. In addition the ZSI provides a simple approach for applications of any DC source (photovoltaic cell, or fuel cell, battery, and diode rectifier) [4, 5].

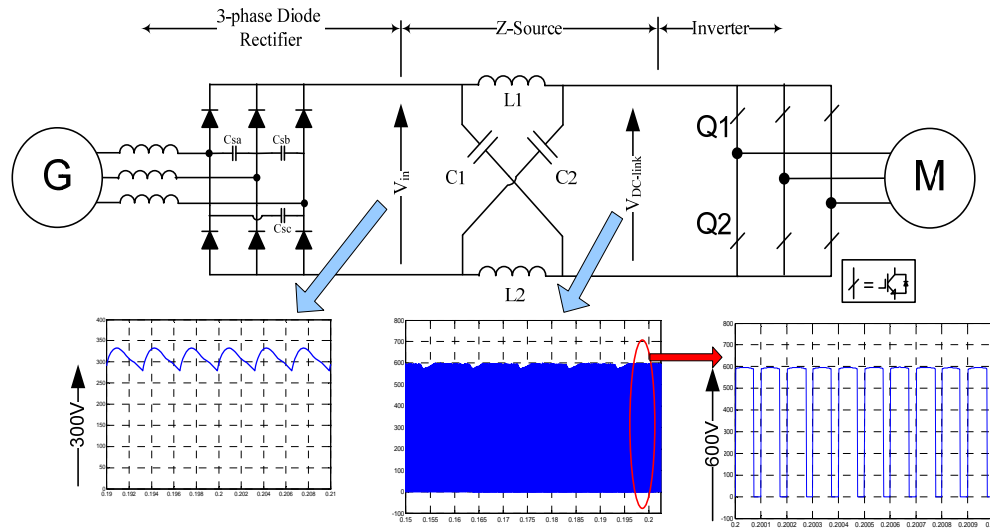
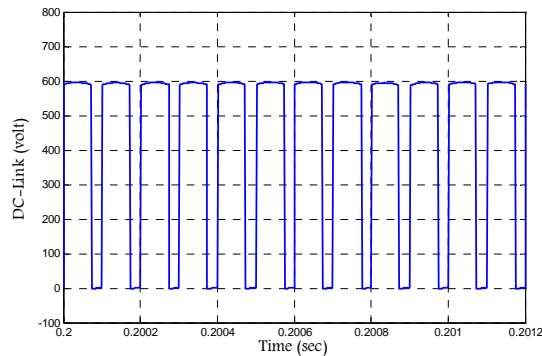


Figure (1) Z-Source Inverter

Unfortunately the control strategies of the output voltage of the Z-source tend to be somewhat complex. This complexity comes from the discontinuous behavior of the output DC-link voltage as shown in fig. (2). Obviously, during the shoot through operating mode the DC-link voltage being zero. While, during the normal (or active) operation the DC-link voltage energized to the desired value. Therefore, this discontinuous DC voltage cannot be used as a feedback signal to control the output voltage. In the literatures, there are two main types of controllers: direct control and indirect control. The direct controller controls the capacitor voltage which cannot govern the output voltage within the desired limit and the DC-link voltage is open to disturbances coming from the input voltage. Whereas, in the indirect controller the DC-link voltage reproduced by somewhat complex sensing and scaling circuit.



Figure(2) DC-Link Waveform

Nowadays, artificial intelligent system presents powerful controllers in many industrial fields. This paper proposed a novel direct feedback controller without any additional circuits to estimate or reproduce a continuous feedback signal. This controller used the features of the adaptive neuro-fuzzy inference system to overcome the problem of discontinuous feedback. The performance of the Z-source is investigated in this paper for different input voltage variation and disturbance.

Mathematical modeling of Z-source Inverter:

Equivalent Switching Circuit of ZSI:

The two non-zero operation modes of the ZSI network involving two different circuit topologies, these two circuits can be summarized in one equivalent circuit which can represents the ZSI operation modes as shown in fig. (3).

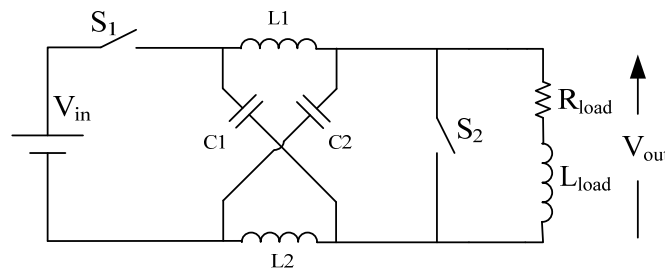


Figure (3) Equivalent Switching Circuit of ZSI Network

In mode-1; S_1 -off and S_2 -on, there is no energy transferred from the source to the load, because the load side and source side are essentially decoupled by the shoot-through state and the open states of S_1 .

In mode-2; S_1 -on and S_2 -off, the real energy will be transferred from the source to the load due to the conduction of S_1 and absence of shoot-through state.

Both of control-to-output and disturbance-to-output voltage transfer functions can be obtained by using small signal modeling based on the following assumptions: the ZSI is operating in continuous condition mod, the passive components in the Z-network are lossless and the load current is continuous because of an inductive load. The AC side circuit can be simplified to an equivalent DC load $Z_{load} = R_{load} + j\omega L_{load}$; where R_{load} is calculated by power balance as $R_{load} = 8|Z_{load}|/3\cos\phi$ and L_{load} is determined so that the time constant of the DC load is the same as the AC load [6].

The state variables of the system can be defined as: $i_{L1}(t)$, $i_{L2}(t)$, $v_{C1}(t)$, $v_{C2}(t)$. The input voltage $V_{in}(t)$ is independent voltage source. The state space equations of mode-1 can be written as:[7]

$$\begin{bmatrix} L_1 & 0 & 0 & 0 \\ 0 & L_2 & 0 & 0 \\ 0 & 0 & C_1 & 0 \\ 0 & 0 & 0 & C_2 \end{bmatrix} \begin{bmatrix} \nabla i_{L1}(t) \\ \nabla i_{L2}(t) \\ \nabla v_{C1}(t) \\ \nabla v_{C2}(t) \end{bmatrix} = \begin{bmatrix} 0 & 0 & 1 & 0 \\ 0 & 0 & 0 & 1 \\ -1 & 0 & 0 & 0 \\ 0 & -1 & 0 & 0 \end{bmatrix} \begin{bmatrix} i_{L1}(t) \\ i_{L2}(t) \\ v_{C1}(t) \\ v_{C2}(t) \end{bmatrix} \quad \dots (1)$$

Where: ∇ represents d/dt

The state space equations of mode-2 are:

$$\begin{bmatrix} L_1 & 0 & 0 & 0 \\ 0 & L_2 & 0 & 0 \\ 0 & 0 & C_1 & 0 \\ 0 & 0 & 0 & C_2 \end{bmatrix} \begin{bmatrix} \nabla i_{L1}(t) \\ \nabla i_{L2}(t) \\ \nabla v_{C1}(t) \\ \nabla v_{C2}(t) \end{bmatrix} = \begin{bmatrix} 0 & 0 & 0 & -1 \\ 0 & 0 & -1 & 0 \\ 0 & 1 & \frac{Z_{load}}{Z_{load}} & \frac{Z_{load}}{Z_{load}} \\ 0 & -1 & \frac{-1}{Z_{load}} & \frac{-1}{Z_{load}} \end{bmatrix} \begin{bmatrix} i_{L1}(t) \\ i_{L2}(t) \\ v_{C1}(t) \\ v_{C2}(t) \end{bmatrix} + \begin{bmatrix} 1 \\ 1 \\ -1 \\ -1 \end{bmatrix} \frac{V_{in}(t)}{Z_{load}} \quad \dots (2)$$

AC Small Signal Modeling of ZSI Based on State Space Averaging:

The small signal relationship among the state variables is derived by applying small signal perturbations $\tilde{v}_{in}(t)$ to the input voltage, and $\tilde{d}(t)$ to the shoot-through duty ratio (D_1) shown by $v_{in}(t) = V_{in} + \tilde{v}_{in}(t)$ and $d(t) = D_1 + \tilde{d}(t)$ [8]. The perturbations result in small signal variations in the state variables $x = X + \tilde{x}$. Combing mode-1 and mode-2 equations and by using state space averaging method, the averaged matrix is [9]:

$$\begin{bmatrix} L_1 & 0 & 0 & 0 \\ 0 & L_2 & 0 & 0 \\ 0 & 0 & C_1 & 0 \\ 0 & 0 & 0 & C_2 \end{bmatrix} \begin{bmatrix} \nabla \tilde{i}_{L1}(t) \\ \nabla \tilde{i}_{L2}(t) \\ \nabla \tilde{v}_{C1}(t) \\ \nabla \tilde{v}_{C2}(t) \end{bmatrix} = \begin{bmatrix} 0 & 0 & D_1 & -D_2 \\ 0 & 0 & -D_2 & D_1 \\ -D_1 & D_2 & \frac{-D_2}{Z_{load}} & \frac{-D_2}{Z_{load}} \\ D_2 & -1 & \frac{-D_2}{Z_{load}} & \frac{-D_2}{Z_{load}} \end{bmatrix} \begin{bmatrix} \tilde{i}_{L1}(t) \\ \tilde{i}_{L2}(t) \\ \tilde{v}_{C1}(t) \\ \tilde{v}_{C2}(t) \end{bmatrix} + \begin{bmatrix} \frac{D_2}{Z_{load}} \\ \frac{D_2}{Z_{load}} \\ \frac{D_2}{Z_{load}} \\ \frac{D_2}{Z_{load}} \end{bmatrix} V_{in}(t) + \begin{bmatrix} V_{C1} + V_{C2} - V_{in} \\ V_{C1} + V_{C2} - V_{in} \\ -I_{L1} - I_{L2} + \frac{V_{C1}}{Z_{load}} + \frac{V_{C2}}{Z_{load}} + \frac{V_{in}}{Z_{load}} \\ -I_{L1} - I_{L2} + \frac{V_{C1}}{Z_{load}} + \frac{V_{C2}}{Z_{load}} + \frac{V_{in}}{Z_{load}} \end{bmatrix} \tilde{d}(t) \quad \dots (3)$$

Where:

D_1 is mode-1 duty cycle, D_2 mode-2 duty cycle, I_{L1} , I_{L2} , V_{C1} , V_{C2} and V_{in} are DC steady state values.

Taking Laplace transformation and solving of the above equations, the capacitor output voltage can be derived [9]:

$$\tilde{v}_c(s) = G_{V_{C/d}}(s) \cdot \tilde{d}_1(s) + G_{V_{C/in}}(s) \cdot \tilde{v}_{in}(s) \quad \dots (4)$$

Where:

$$G_{V_{C/d}}(s) = \left. \frac{\tilde{v}_c(s)}{\tilde{d}(s)} \right|_{\tilde{v}_{in}=0} = \frac{(-2 I_L + \frac{2V_C - V_{in}}{R_{load}})LS + (D_2 - D_1) \cdot (2V_C - V_{in})}{LCS^2 + \frac{2D_2L}{Z_{load}}S + (D_1 - D_2)^2} \quad \dots (5)$$

And

$$G_{V_{C/in}}(s) = \left. \frac{\tilde{v}_c(s)}{\tilde{v}_{in}(s)} \right|_{\tilde{d}(s)=0} = \frac{\frac{D_2L}{Z_{load}}S + D_2(D_2 - D_1)}{LCS^2 + \frac{2D_2L}{Z_{load}}S + (D_1 - D_2)^2} \quad \dots (6)$$

Substituting $Z_{load}(s) = R_{load} + s L_{load}$ gives:

$$G_{V_{c/d}}(s) = \frac{b_0 s^2 + b_1 s + b_2}{a_0 s^3 + a_1 s^2 + a_2 s + a_3} \quad \dots(7)$$

$$G_{V_{c/in}}(s) = \frac{h_0 s + h_1}{a_0 s^3 + a_1 s^2 + a_2 s + a_3} \quad \dots (8)$$

Where:

$$a_0 = L L_{load} C$$

$$a_1 = R_{load} L C$$

$$a_2 = 2 D_2 L + L_{load} (D_1 - D_2)^2$$

$$a_3 = R_{load} (D_1 - D_2)^2$$

$$b_0 = (-2 L_{load} + \frac{2 V_c - V_{in}}{R_{load}}) \cdot L \cdot i_L$$

$$b_1 = -2 R_{load} L I_{load} + (2 V_c - V_{in}) \cdot L + (2 V_c - V_{in}) (D_2 - D_1) i_{load}$$

$$b_2 = (D_2 - D_1) \cdot (2 V_c - V_{in}) \cdot R_{load}$$

$$h_0 = D_2 (D_2 - D_1) L_{load} + D_2 L$$

$$h_1 = D_2 (D_2 - D_1) R_{load}$$

Control Strategies:

Voltage mode closed loop control is used to control the output voltage of the ZSI to the desired value. A feedback signal from the DC-link voltage of Z-source inverter achieves the good reference tracking and disturbance rejection. Since the Z-source network has RHP zero in the control-to-output transfer function which is resulting in non-minimum phase response. Therefore, improve the complex of the control design, and deteriorate the dynamic response [10].

Indirect Control of ZSI:

The DC-link voltage v_{out} is the square waveform due to the operating modes. This has zero value during the shoot-through state and it has peak value v_{out} during non-shoot-through state. Therefore, the peak DC-link voltage is not suitable to be used as a feedback signal [10]. Most papers used the Z-source capacitor voltage as a feedback, because of its continuity, to estimate the error signal between the capacitor voltage and reference value, and then control the duty ratio d_1 through PID controller to obtain constant capacitor voltage as shown in fig. (4). It is obvious that by controlling only the capacitor voltage, the DC-link voltage is open to disturbances coming from the input voltage. This effect could be transferred to the output side, which distorts the output voltage and increase the output voltage stress across the switches.

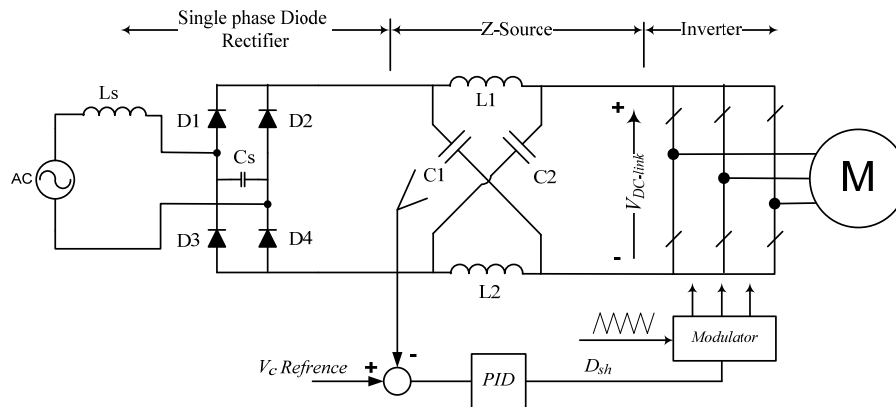


Figure (4) Indirect Control of ZSI

Direct Control of ZSI:

The peak DC-link voltage which has a square waveform can be measured (or detect) by using a peak detection circuit. The measurement signal, which is no more pulsating, can be used as a feedback signal as shown in fig. (5). The non-zero value of the dc-link voltage $v_{dc-peak}$ (peak dc-link voltage) is a linear combination of the capacitor voltage which is state variable and the input voltage ($v_{dc-peak} = 2v_c - v_{in}$) [11]. In steady state operation the capacitor voltage and the input voltage are continuous signals. Although the DC-link voltage $v_{dc-link}$ itself is a pulsating waveform, the peak value of the DC-link voltage $v_{dc-peak}$ can be obtained as a continuous signal.

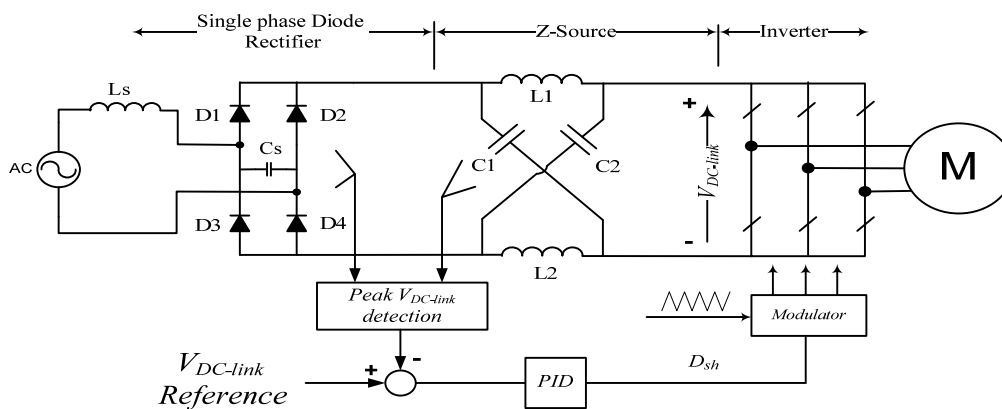


Figure (5) Direct Control of ZSI

Adaptive Neuro-Fuzzy System:

Since fuzzy logic (FL) was introduced by Lotfi Zadeh in 1965, it had many successful applications mostly in control. One of the main advantages of fuzzy logic system is the design on the basis of incomplete and approximate information, thus providing simple and fast approximations of the unknown or too complicated models [12, 13]. Sugeno fuzzy-control technique belongs to the robust controller category, which deals with model uncertainties of simplified model. These uncertainties may come from un-modeled dynamics, variations in system parameters, or approximations of complex plant behaviors. Fuzzy-control is a powerful approach to solve system state tracking problems [13, 14].

The design of the Membership Functions (MFs) and the rules table of a fuzzy inference system were based on the experience of the operator or designer of the system. This means that there is no systematic method for design of a fuzzy system. On the other hand, in a neural network the experimental or simulation input/output data can be used to train a network. The network then represents the model which satisfies that data. These techniques can be brought into a hybrid neuro-fuzzy system to build a more powerful intelligent system with improved design and performance features called Adaptive Neuro-Fuzzy Inference System ANFIS [15]. As name indicates, a fuzzy inference system is designed systematically using the neural network design method. This means that if the desired input/output data patterns are available for a fuzzy system, the MFs and rules table can be designed using the neural network training method.

Usually the sugeno method is used in adaptive neuro-fuzzy system. For example: if X & Y are the inputs of the fuzzy system, and "F" is the output signal:

IF X is A₁ AND Y is B₁ THEN z=f₁

IF X is A₂ AND Y is B₂ THEN z=f₂

The output "F" can be constructed as:

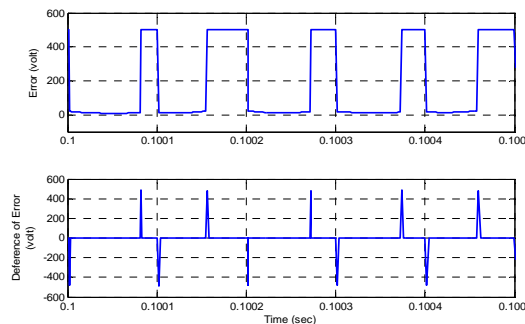
$$F = \frac{W_1}{W_1+W_2} f_1 + \frac{W_2}{W_1+W_2} f_2 \quad \dots(9)$$

Where

A₁, A₂, B₁, B₂ are the input MFs, f₁ and f₂ are the output singleton MFs, and W₁ and W₂ are the Degree Of Fulfillments (DOF) of rule 1 & 2, which can be adaptive by using any training algorithm to satisfied the input/output data [15].

Design of an Adaptive Neuro-Fuzzy Controller:

A discrete adaptive neuro-fuzzy controller can be implemented to control the output D.C link voltage of Z source inverter. This type of controller can be adapted to modify the discontinuous feedback signal of the output D.C link voltage to satisfy the input reference command signal. The ANFIS controller has two input signals; first is the discrete error signal between the actual DC-link and the desired value. And the second is the deference signal between the instant plant error e(k) and the previous plant error e(k-1). These two signals are the inputs of the fuzzy system as shown in fig. (6):



Figure(6) input signal to the ANFIS controller

Which must recognize the state of the system and predicts a suitable linear feedback signal $f(k)$. According to that function of the fuzzy controller, an adaptive controller of two inputs and three- Gaussian type MFs of each input is used in this work. The output MFs and rules are adapted by using neural training algorithm of large number of input/output data patterns obtained from the conventional direct PID controller. The adaptive neuro-fuzzy system parameters input/output memberships, rules and surface performance are shown in fig. (7). The accuracy performance of the designed neuro-fuzzy inference system between the desired output and fuzzy output is shown in fig. (8). The overall system simulation of the ANFIS controller is shown in fig. (9) and the switching model based on the modified space vector pulse width modulation (MSVPWM) technique is shown in fig.(10)

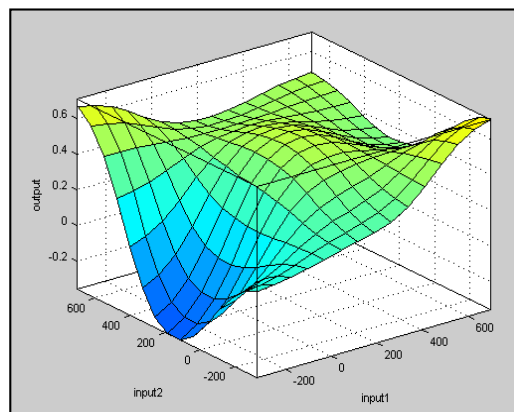


Figure (7) Inputs/Output Surface Performance of The ANFIS Controller.

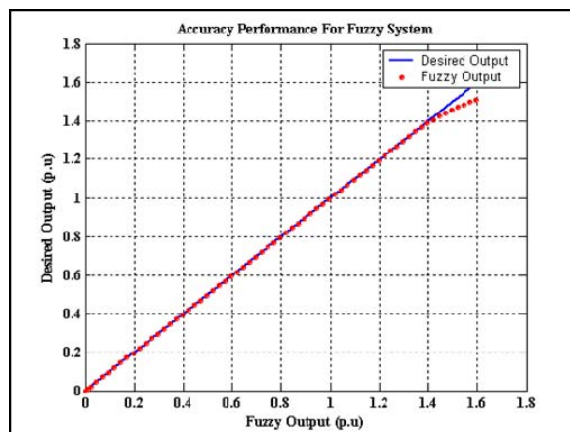


Figure (8) Accuracy Performance for Fuzzy System

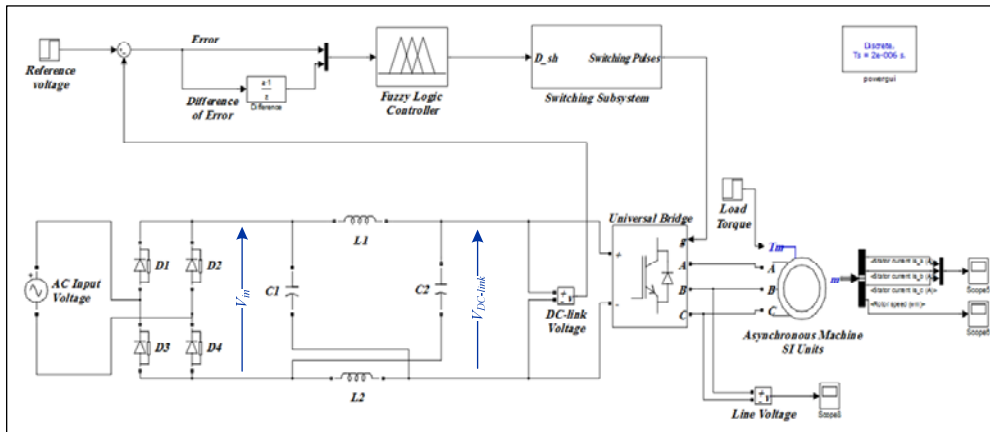


Figure (9) System Simulation

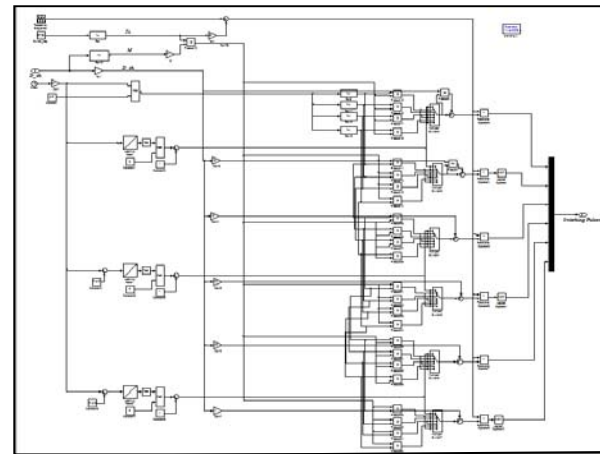


Figure (10) Switching Subsystem Based on MSVPWM Technique

Simulation Results:

Simulation results have been carried out to improve the concept and verify the features of the proposed adaptive neuro-fuzzy inference system direct control of the Z-source Inverter as a three-phase induction motor drive system. System parameters used in the simulation are: $V_{in}=220\text{rms}$, $C=470\mu\text{F}$, $L=250\mu\text{H}$, $D=0.3$, switching frequency=10kHz, I.M: 3- ϕ , 7 hp, 400V, 50Hz, 4-pole induction motor. Figure (11) shows the DC-link and the capacitor voltages performances for different input command reference values. Obviously, in this method the DC-link voltage tracks the command reference with approximately zero rise-time, over-shoot and steady state error. While, the capacitor voltage is still uncontrolled and free to disturbance as in 0.3 sec. voltage sag.

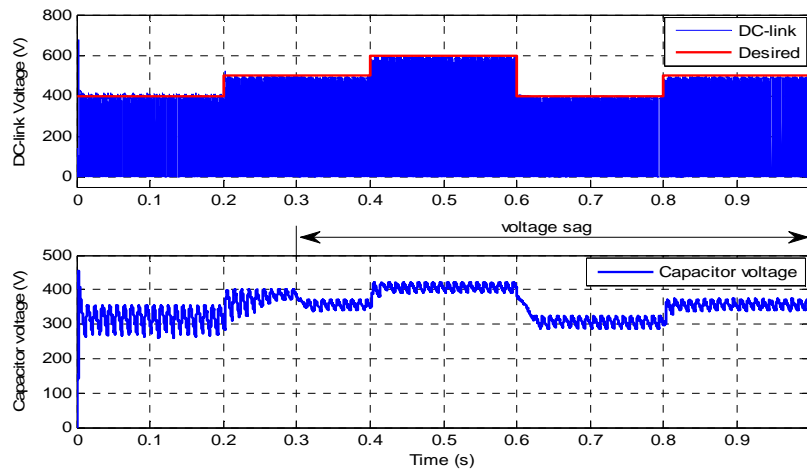


Figure (11) The output DC-link voltage tracking and the capacitor voltage

Figure (12) shows the simulation performance of the DC-link and capacitor voltages in case of 20% input voltage sag at 0.3 sec. with ANFIS direct control. It can be seen that the DC-link voltage is maintained fix at the desired value during the voltage sag, and the voltage ripple is partly eliminated by the control loop. Figure (13) shows the AC output side performance: voltage, motor current and motor speed during the period of 20% input voltage sag. It's clear that the AC voltage maintained constant but the capacitor voltage increases during disturbance. Also the motor current and hence torque and speed are stable and fixed during voltage sag. In addition, figure (14) shows the DC and AC sides performance under 40% input voltage sag. Obviously, the ANFIS controller successes to overcome the voltage sag and maintain the DC-link voltage at the desired value, and hence obtained stable AC voltage and speed.

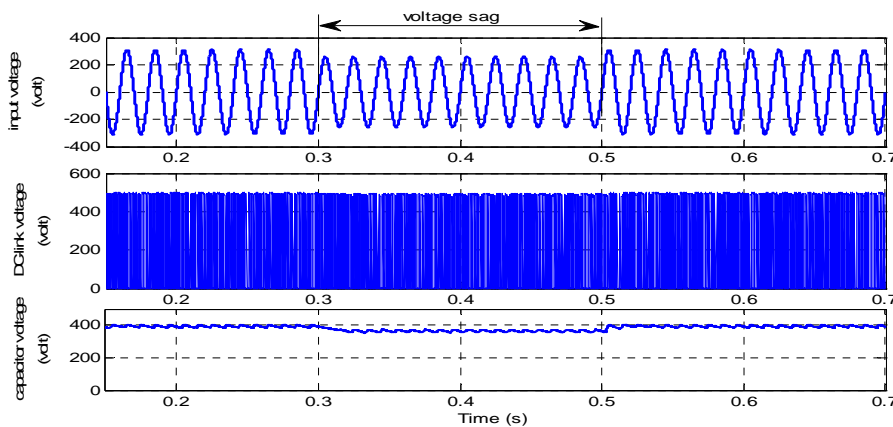


Figure (12) DC-link and Capacitor Voltages Under 20% Voltage Sag

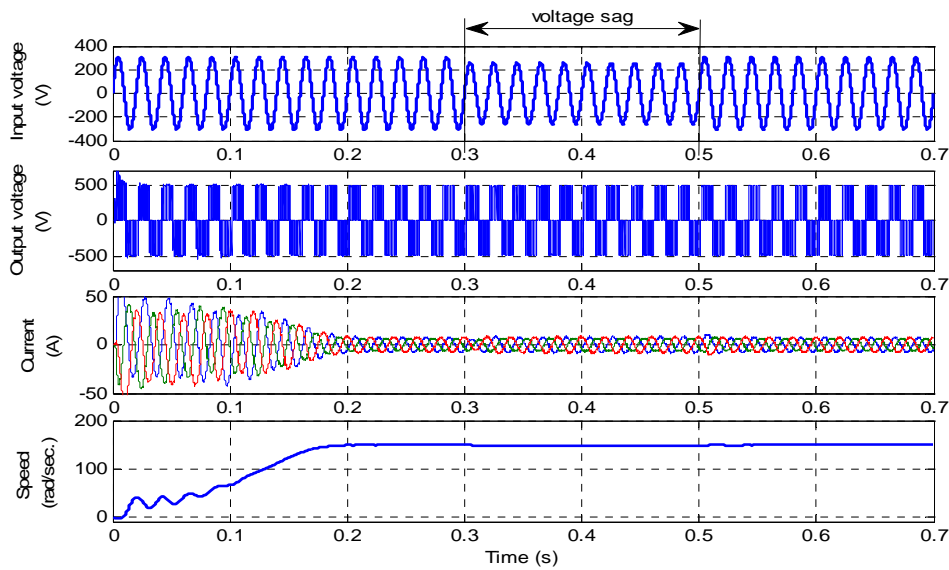


Figure (13) Output AC Side Performance Under 20% Voltage Sag

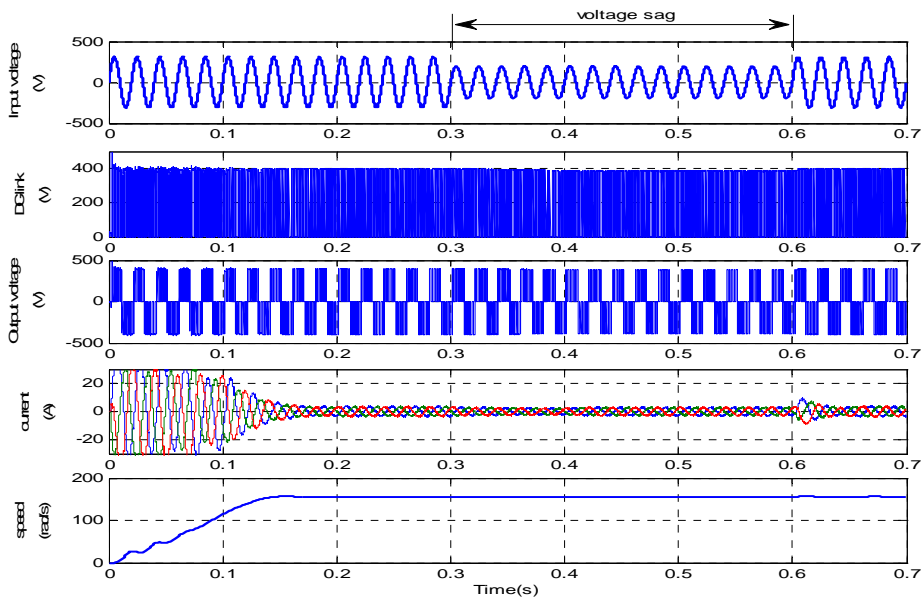


Figure (14) System Performance Under 40% Voltage Sag

In order to realize the features of the proposed ANFIS direct controller, a comparison between its performance and the conventional control methods is represented. Figures (15) and (16) show the performance of traditional indirect and direct controllers of the ZSI respectively. In the case of direct controller the DC-link is controlled to the desired value but with higher peak ripple and higher cost and complexity of using additional estimation circuits. Whereas, in the case of indirect control the cost and complexity are reduced but the controller fixes the capacitor voltage and leave the DC-link voltage free to disturbance. In this method the DC-link

and the AC voltage are uncontrolled and increased during voltage sag period, which may causes saturation of motor stator due to current increasing as shown in fig. (17).

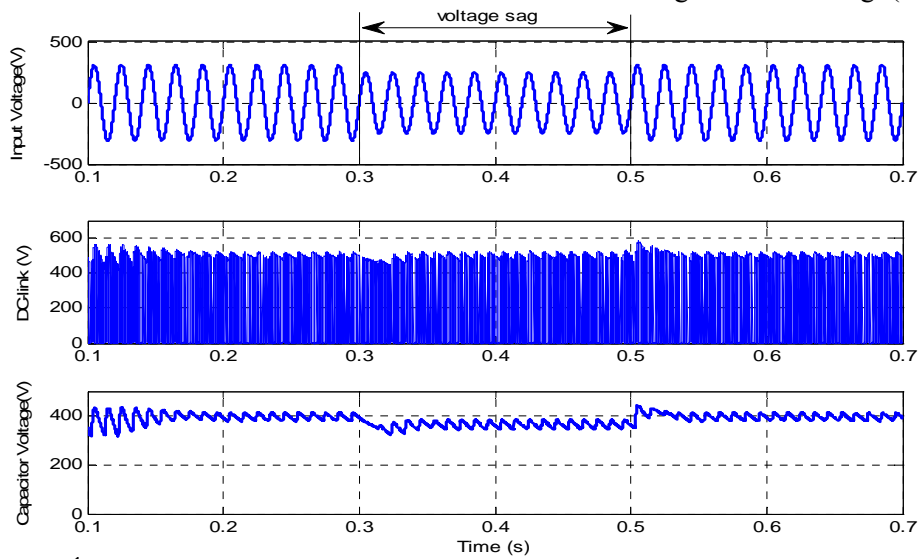


Figure (15) DC-link and Capacitor Voltages Under 20% Voltage Sag of the Conventional Direct Controller

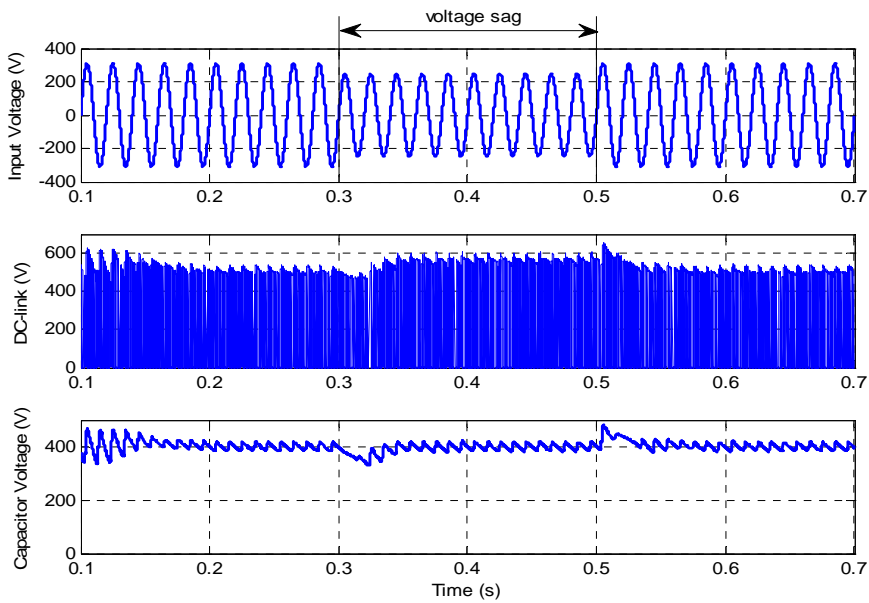


Figure (16) DC-link and Capacitor Voltages Under 20% Voltage Sag of the Indirect Controller

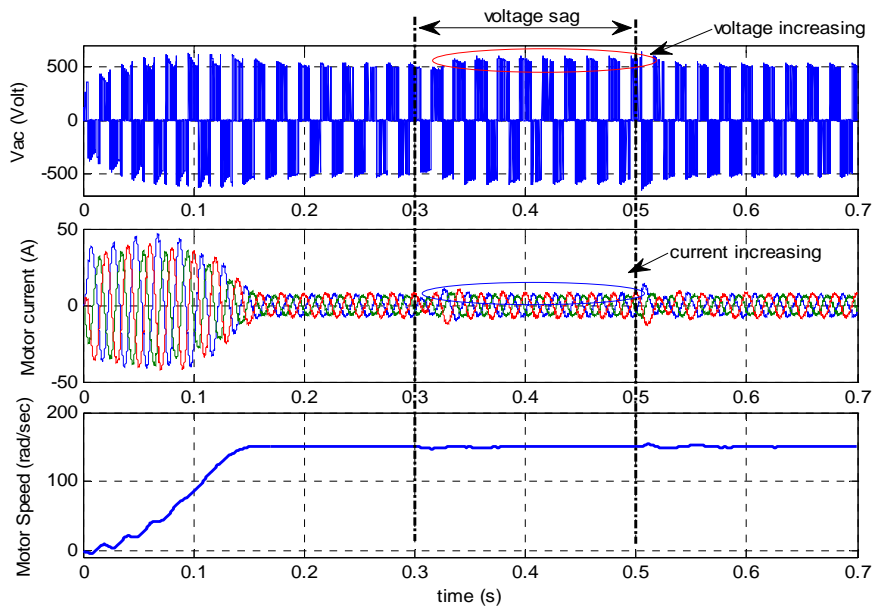


Figure (17) AC Side Performance of the conventional Controller

CONCLUSION:

In this paper a novel direct control of the Z-source inverter is proposed, the description of the adaptive neuro-fuzzy inference controller is illustrated, the features of the proposed controller are demonstrated stimulatingly. Obviously, simulation results show that the proposed direct controller of Z-source inverter has an excellent performance of the output voltage compared with conventional methods. The main contribution of the proposed method is reduced the complexity of the controller by the absence of complex estimation circuits, and obtained ripple free DC-link voltage. It can be seen clearly that the output DC-link of the Z-source inverter tracks the desired value under full-load condition and 20% input voltage sag as illustrated in fig. (11). Moreover, results show that the artificial controller can overcome any disturbance in the input line. A 20% and 40% voltage sag cases in the input voltage are not affect the DC-link voltage which maintains constant at the desired value by the action of the ANFIS controller. Consequently, the output AC voltage of the inverter obtained constant and gives a stable operation and speed of the induction motor drive under constant torque condition as shown figs. (12, 13 and 14). As conjunction with conventional control methods the proposed direct controller in this paper not only eliminates the DC-link ripple but reduces the complexity of the controller by omits any additional estimation or peak detection circuit.

REFERENCES:

[1] Fang Zheng Peng; "Z-source inverter", Industry Applications, IEEE Transactions on, Volume: 39 Issue: 2, Mar/Apr 2003, Page(s):504-510.
 [2] Singh, C.S.; Tripathi, R.K., "Maximum constant boost control of switch inductor quasi Z-source inverter," Engineering and Systems (SCES), 2013 Students Conference on, vol., no., pp.1,5, 12-14 April 2013.
 [3] Vrushali Suresh Neve; P.H. Zope; S.R. Suralkar; "A Literature Survey On Z-Source Inverter", VSRD International Journal of Electrical, Electronics & Communication Engineering, Vol. 2 No. 11 November 2012.

- [4] Peng, F.Z; Xiao-ming Yuan; Xu- Fang; Zhao-ming Qian; “Z-source inverter for adjustable speed drives”, Power Electronics Letters, IEEE, Volume: 1 Issue: 2, June 2003, Page(s): 33 –35.
- [5] Majid K. Al-Khatat, "Analysis of Z-Source Inverter For Space Vector PWM Fed 3-Phase Induction Motor", Engineering & Technology Journal ISSN: 24120758, Volume 28, Issue 17, Page 5440-5454, 2010.
- [6] Miaosen Shen, Qingsong Tang, Fang Zheng Peng, “Modeling and Controller Design of the Z-Source Inverter with Inductive Load”, IEEE Power Electronics Specialists Conference, PESC 2007, pp: 1804-1809.
- [7] O. Ellabban, V. Mierlo and Philippe Lataire, "Voltage Mode and Current Mode Control for a 30 kW High-Performance Z-Source Inverter", IEEE Electrical Power & Energy Conference, 2009.
- [8] R. W. Erickson and D. Maksimovic, "Fundamentals of Power Electronics", 2nd ed. Norwell, MA: Kluwer, 2001.
- [9] Jingbo Liu, Jiangang Hu, and Longya Xu, "Dynamic Modeling and Analysis of Z Source Converter—Derivation of AC Small Signal Model and Design-Oriented Analysis", IEEE TRANSACTIONS ON POWER ELECTRONICS, VOL. 22, NO. 5, SEPTEMBER 2007.
- [10] Xinpeng Ding, Zhaoming Qian, Shuitao Yang, Bin Cui, Fangzheng Peng, " A PID Control Strategy for DC-link Boost Voltage in Z-source Inverter", IEEE , p.1145, 2007.
- [11] Xinpeng Ding, Zhaoming Qian, Shuitao Yang, Bin Cui, Fangzheng Peng, " A Direct DC-link Boost Voltage PID-like Fuzzy Control Strategy in Z-Source Inverter", IEEE, p.405, 2008.
- [12] K. M. Passino and S. Yurkovich, "Fuzzy control", Addison – Wesley Longman, 1998.
- [13] Fadhil A. Hassan, Lina J. Rashad, Fatma H. Faris, "An Adaptive Fuzzy Inference System for 3-Phase Synchronous Generator Excitation Control", Engineering & Technology Journal ISSN: 24120758, Volume 28, Issue 20, Pages 6050-6060, 2010.
- [14] C. C. Wong and B. C. Hung, "Genetic-Based Sliding Mode Fuzzy Controller Design", Tamkang Journal of Science and Engineering, Vol.4, No.3, 2001.
- [15] R. Jang, “Input selection for ANFIS learning” in Proc. 5th IEEE Int. Conf. Fuzzy Systems, Sep. 8–11, 1996, vol. 2, pp. 1493–1499.